

# Generation of Chaotic Signals With Concealed Time-Delay Signature Based on a Semiconductor Laser Under Multi-Path Optical Feedback

Bing Cui, Guangqiong Xia<sup>✉</sup>, Xi Tang, Fei Wang<sup>✉</sup>, Zaifu Jiang, Yanfei Zheng, Fengling Zhang, and Zhengmao Wu<sup>✉</sup>

**Abstract**—A simple scheme for generating chaotic signals with concealed time-delay signature (TDS) is proposed and experimentally demonstrated. The architecture of the system is based on a semiconductor laser (SL) under multi-path optical feedback (MPOF) provided by a  $2 \times 2$  fiber coupler (FC) and a fiber mirror (FM). The results show that SLs with MPOF are more beneficial for achieving TDS suppressed chaotic output than those with single optical feedback (SOF) systems. In addition, the TDS of the chaotic signal generated by the SL under MPOF is insensitive to the length deviation of the feedback cavities, and therefore such a scheme is convenient for practical application. Furthermore, the influence of FC coupling ratio in the MPOF module, feedback strength, and bias current of the SL on the TDS is comprehensively studied. By selecting suitable parameters, the TDS of the chaotic signal generated by the SL under MPOF can be completely concealed. Finally, permutation entropy (PE) is adopted to evaluate the complexity of the generated chaotic signal, and the result demonstrates that the suppression of TDS does not lead to the degradation of complexity for the proposed scheme.

**Index Terms**—Chaos, multi-path optical feedback (MPOF), semiconductor laser (SL), time-delay signature (TDS).

## I. INTRODUCTION

OPTICAL chaotic sources based on semiconductor lasers (SLs) under various external perturbations such as optical feedback [1]–[7], optical injection [8]–[11], and optoelectronic feedback [12], have received great attention because of their important applications in secure communication [13], random bits generation [14], [15], optical sensors [16], range radar [17], etc. Among these chaotic sources, external cavity semiconductor lasers (ECSLs) attract extra concern because of their abundant dynamic characteristics and compatibility with optical communication systems [18]. However, the chaotic signal from an

Manuscript received November 1, 2021; revised November 29, 2021; accepted December 6, 2021. Date of publication December 10, 2021; date of current version December 20, 2021. This work was supported in part by the National Natural Science Foundation of China under Grants 61775184 and 61875167. (*Corresponding authors:* Guangqiong Xia; Zhengmao Wu.)

Bing Cui, Guangqiong Xia, Xi Tang, Fei Wang, Yanfei Zheng, Fengling Zhang, and Zhengmao Wu are with the School of Physical Science and Technology, Southwest University, Chongqing 400715, China, and also with the Chongqing Key Laboratory of Micro & Nano Structure Optoelectronics, Southwest University, Chongqing 400715, China (e-mail: cuibing524@126.com; tx1982@swu.edu.cn; tx1982@swu.edu.cn; wangf17@swu.edu.cn; yfzhengswu@163.com; 582266566@qq.com; zmwu@swu.edu.cn).

Zaifu Jiang is with the School of Mathematics and Physics, Jingchu University of Technology, Hubei 448000, China (e-mail: jiangzaifu23003@163.com).

Digital Object Identifier 10.1109/JPHOT.2021.3133659

ECSL usually possesses obvious time-delay signature (TDS) [19]–[21], which will degrade the performances of precision in ranging, randomness in bits generation, and security in chaos-based communications. The simplest method for weakening the TDS in an ECSL system is to decrease the feedback strength [22]. However, the complexity of the generated chaotic signal is relatively low under low feedback strength [23]. In order to solve this issue, one scheme based on two external cavities is proposed by adding another external cavity. For two external cavities with proper feedback strength, the TDS of the generated chaotic signals can be successfully suppressed when the difference of the flying time of light within two external cavities is equal to half of the period of relaxation oscillation [24]. As a result, the length of one of the two cavities should be controlled precisely, which is relatively difficult for implementation. Additionally, relevant theoretical investigation demonstrates that, via parallel coupling ring resonators to provide nonlinear filtering feedback, the TDS of the generated chaotic chaos can also be suppressed effectively [25].

In this paper, we proposed and experimentally demonstrated a simple system for generating the chaotic signal with concealed TDS. The scheme is based on a SL under multi-path optical feedback (MPOF). In such a system, the MPOF module is mainly composed of a fiber coupler (FC) and a fiber mirror (FM). Through inspecting the influence of some operating parameters on the TDS of the generated chaotic signal, we find that the bias current, the coupling ratio of the FC in MPOF module and the feedback strength have a severe impact on the TDS of the chaotic signal. However, the TDS of the generated chaotic signal is insensitive to the length of the feedback cavity, which is very convenient for practical applications. Through mapping the TDS in the parameter space of the bias current and the feedback strength, the optimized parameter region for generating chaotic signals with TDS below 0.1 is determined. Moreover, via the permutation entropy (PE) to analyze the complexity of the generated chaotic signal [23], the complexity of the chaotic signal does not decrease while the TDS is successfully concealed.

## II. EXPERIMENTAL SETUP

The experimental setup is presented in Fig. 1. A distributed feedback SL is used as a laser source, and the bias current and temperature of the SL are controlled by a laser driver and

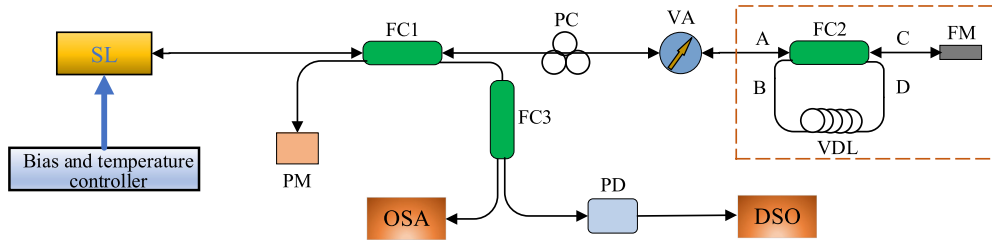


Fig. 1. Experimental setup. SL: semiconductor laser, PM: power meter, FC: fiber coupler, PC: polarization controller, VA: variable attenuator, VDL: variable delay line, FM: fiber mirror, OSA: optical spectrum analyzer, DSO: digital oscilloscope.

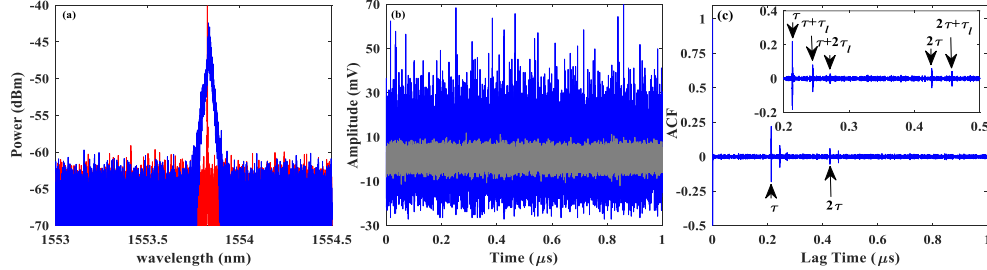


Fig. 2. Optical spectrum (a) time series, (b) and ACF (c) of the SL output for FC2 of an 80/20 coupling ratio, where the bias current is  $1.4 I_{th}$ , the feedback strength is 17.0%, and  $L_{VDL} = 3.35$  m. The red curve is the optical spectrum of the free-running SL.

temperature controller (ILX-Lightwave, LDC-3724). During the experiment, the temperature of the SL is stabilized at  $20.00^{\circ}\text{C}$ . Under this case, the threshold current of the SL is about 9.1 mA. The output light of the SL is split into two parts by a 90/10 fiber coupler (FC1). One with the 90.0% emitting optical power is sent to a MPOF module after passing a polarization controller (PC) and a variable attenuator (VA). The MPOF module is composed of a  $2 \times 2$  fiber coupler (FC2), a FM, and a variable delay line (VDL). For comparison, single optical feedback (SOF) can be implemented if emptying the terminal B and D of the FC2, and the corresponding feedback time is marked as  $\tau$ . In this experiment,  $\tau$  is fixed at 213.1 ns. Linking a VDL to terminal B with D, the MPOF is achieved. The additional delayed time resulting from the VDL is marked as  $\tau_l$ , which can be adjusted through varying the length of the VDL ( $L_{VDL}$ ). The other 10.0% SL optical power after FC1 is sent to the measurement system after passing through FC3. An optical spectrum analyzer (OSA, Aragon Photonics BOSA lite +, 20MHz resolution) is used to observe the optical spectrum distribution. A digital oscilloscope (OSC, Agilent DSO-X91604A, 16 GHz bandwidth) with a photodetector (PD, New Focus 1544B, 12 GHz bandwidth) is utilized to record the time series. The feedback strength is defined as the ratio of the feedback power to the output power of the free-running SL [26], where the feedback power is measured by a power meter (PM) through a port of FC1.

### III. RESULTS AND DISCUSSION

The TDS of a chaotic signal can be analyzed by calculating the autocorrelation function (ACF) of the time series, which is defined as follows:

$$C(\Delta t) = \frac{\langle [I(t + \Delta t) - \langle I(t + \Delta t) \rangle][I(t) - \langle I(t) \rangle] \rangle}{\sqrt{\langle [I(t + \Delta t) - \langle I(t + \Delta t) \rangle]^2 \rangle \langle [I(t) - \langle I(t) \rangle]^2 \rangle}}, \quad (1)$$

where  $I(t)$  represents the output time series,  $\langle \cdot \rangle$  denotes the time average, and  $\Delta t$  is the time shift.

The complexity of a time series is evaluated by the PE [27], which is defined as follows: the time series  $\{I(i), i = 1, 2, \dots, N\}$  are firstly reconstructed into a set of  $m$ -dimensional vectors after choosing an appropriate embedding dimension  $m$  and an embedding delay time  $\tau_e$ . Every vector belongs to one particular order permutation for the  $m$  intensities, amongst the total of  $m!$  possible permutations. For a permutation labeled as  $s$ , its number of occurrences is denoted by  $p(s)$ , which is normalized to the total number of vectors. PE is then defined as:

$$H[P] = \frac{-\sum p(s)\log p(s)}{\log(m!)}. \quad (2)$$

The value of  $H[P]$  ranges from 0 to 1. The higher the value of  $H$  is, the higher the complexity of the chaotic signal is. During calculating PE,  $m$  and  $N$  are set at 6 and 80000, respectively.

Fig. 2 displays the experimental measured optical spectra, time series and corresponding ACF curves for the SL subject to MPOF.

Here, FC2 with an 80/20 coupling ratio is adopted first, the bias current of the SL is  $1.4 I_{th}$ , the feedback strength is 17.0%, and the length of VDL is 3.35 m. As shown in this diagram, the optical spectrum (blue) is obviously widened compared with that of the SL at free-running (red), and the time series in Fig. 2(b) varies erratically. Combining the time series and optical spectra, it can be determined that the output waveforms are chaotic. For the ACF curve shown in Fig. 2(c), there are several peaks emerging at  $N\tau + n\tau_l$  ( $N = 1, 2, n = 0, 1, 2$ ), where  $\tau$  is the feedback time under SOF and  $\tau_l$  is the additional delay introduced by the VDL. It should be noted that the location of the highest peak in the ACF is dependent on the coupling ratio of FC2. Therefore, in the following discussion, apart from the peaks resulting from the relaxation oscillation, the highest peak in ACF is selected to characterize the TDS.

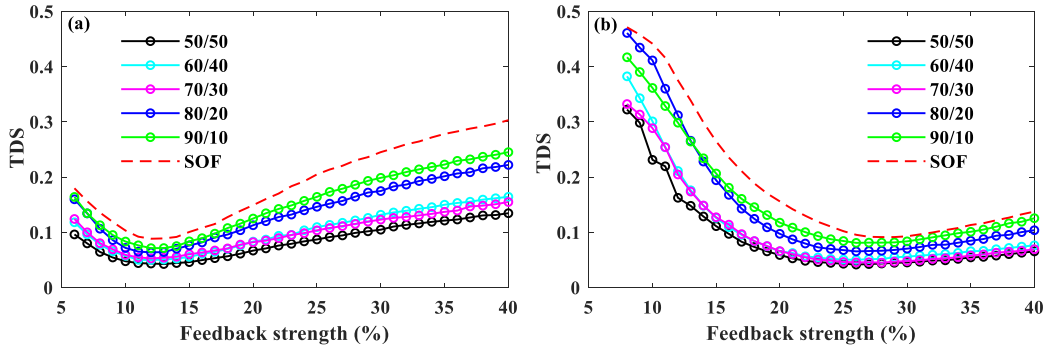


Fig. 3. TDS of the output chaotic signal as a function of feedback strength for the SL biased at  $1.1 I_{th}$  (a)  $1.4 I_{th}$  and (b) under MPOF with  $L_{VDL} = 3.35$  m. Different colors represent the FC2 with different coupling ratios, and every circle represents the average of 20 measurements for each time series with  $10 \mu s$ .

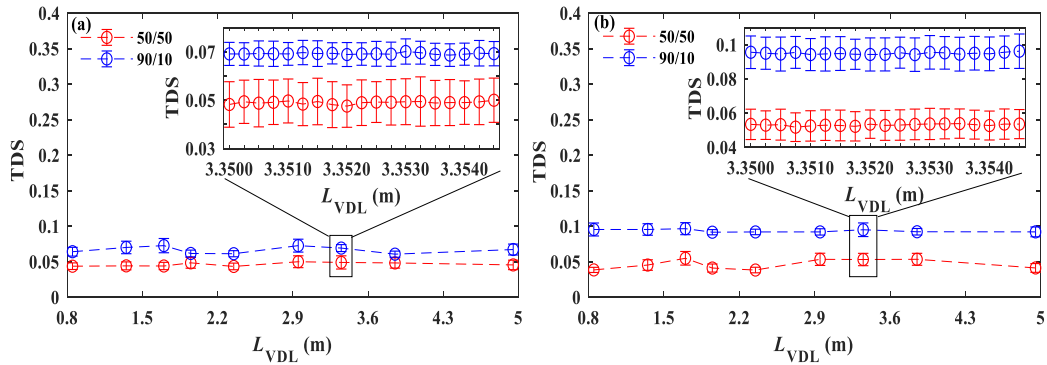


Fig. 4. TDS of the output chaotic signal as a function of  $L_{VDL}$  for the SL biased at  $1.1 I_{th}$  with 12.0% feedback strength (a) and the SL biased at  $1.4 I_{th}$  with 23.0% feedback strength. (b) under MPOF with a 50/50 FC2 (red) and a 90/10 FC2 (blue). Every circle and error bar represents average value and standard deviation, respectively.

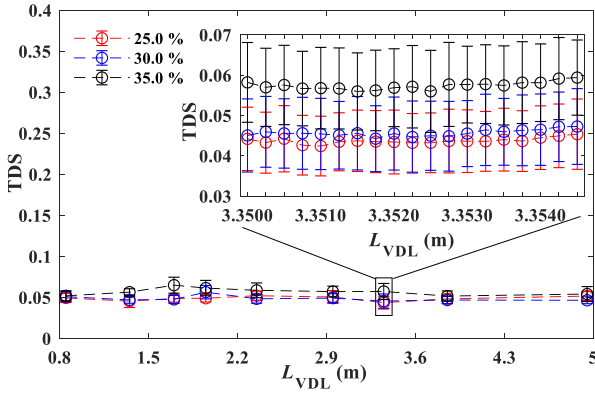


Fig. 5. TDS of the output chaotic signal as a function of  $L_{VDL}$  for the SL biased at  $1.4 I_{th}$  subject to MPOF under a FC2 with 50/50 coupling ratio. Different colors represent different feedback strengths, and every circle and error bar represents average value and standard deviation respectively.

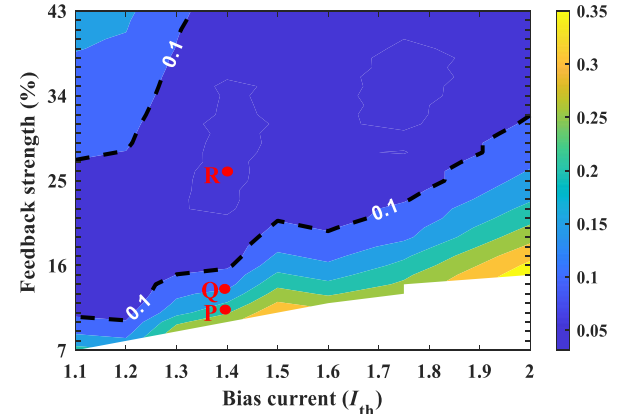


Fig. 6. Map of the TDS of the output chaotic signal in the parameter space of the bias current and feedback strength, where the coupling ratio of the FC2 is 50/50, and  $L_{VDL} = 3.35$  m.

Fig. 3 shows the TDS of the chaotic signal as a function of the feedback strength with different coupling ratios of FC2 when the SL is biased at  $1.1 I_{th}$  and  $1.4 I_{th}$ . Here, the dashed lines are for the SL under SOF, and the solid lines with markers are for the SL under MPOF. From this diagram, it can be seen that, with the increase of the feedback strength, the TDS firstly decreases and then increases for both SOF and MPOF. However, for a given feedback strength, lower coupling ratio of FC2 will be helpful for achieving lower TDS. It can be explained as follows.

With the decrease of the coupling ratio of the FC2, the feedback strength difference among the multi-path of feedback gradually decreases, and therefore the highest peak values of feedback are gradually weakened while the total energy of feedback strength is unchanged. Thus, for different coupling ratios of FC2, the feedback strengths when the TDS gets its minimum are approximately the same and the optimized feedback strengths are about 12.0% for the SL biased at  $1.1 I_{th}$  and 23.0% for the SL biased at  $1.4 I_{th}$  with 50/50 coupling ratio of the FC2. Compared

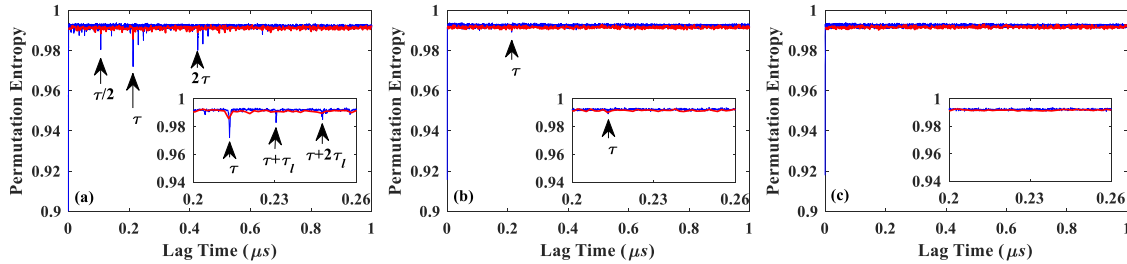


Fig. 7. PE of the output chaotic signal for the SL subject to MPOF under the FC2 with 50/50 coupling ratio and  $L_{VDL} = 3.35$  m, where (a), (b), and (c) represent points P (1.4  $I_{th}$  bias current, 11.0% feedback strength), Q (1.4  $I_{th}$  bias current, 14.0% feedback strength) and R (1.4  $I_{th}$  bias current, 26.0% feedback strength) in Fig. 6, respectively. Blue:  $\tau_e = 0.125$  ns; red:  $\tau_e = 1.875$  ns.

with the case of the SL under SOF, the SL under MPOF is more beneficial for acquiring the chaotic signal with weaker TDS.

As mentioned in [24], in a chaotic system based on a SL subject to two external cavities feedback, the TDS of the generated chaotic signal is very sensitive to the length deviation between the two cavities. In this work, the shortest feedback delay time  $\tau$  is fixed at 213.1 ns (corresponding to about 21.3 m external cavity length), and other feedback times located at  $\tau + n\tau_l$  ( $n = 1, 2, 3 \dots$ ) is varied through adjusting the length of VDL ( $L_{VDL}$ ). Fig. 4 gives the variation of TDS of the generated chaotic signal with  $L_{VDL}$ . Here, we inspect two cases, one is for the SL biased at  $1.1 I_{th}$  with 12.0% feedback strength, and the other is for the SL biased at  $1.4 I_{th}$  with 23.0% feedback strength. Moreover, two FCs with coupling ratios of 90/10 and 50/50 are utilized, respectively. Obviously, for the SL biased at two different values and FC2 with two different coupling ratios, the TDS of the generated chaotic signal is insensitive to  $L_{VDL}$ . In order to examine the influence of tiny variation of  $L_{VDL}$  on the TDS,  $L_{VDL}$  varies from 3.35000 m to 3.35450 m with a step of 0.00025 m, and the results are presented in the insets of Fig. 4. From the insets of Fig. 4, it can be seen that, within a very small scale, the TDS of the generated chaotic signal is still insensitive to  $L_{VDL}$ . The reason is that, compared with SOF, the influence of feedback light phase is weaker for MPOF.

More generally, we consider the case that the feedback strength is taken other values (25.0%, 30.0% and 35.0%), and the corresponding results are given in Fig. 5. Here, the bias current is set at  $1.4 I_{th}$ , and the coupling ratio of the FC2 is 50/50. Obviously, under different feedback strengths, the TDS is still insensitive to the variation of  $L_{VDL}$ , which reveals the cavity length robustness of the proposed multi-path optical feedback scheme on the TDS suppression.

The above results demonstrate the influence of the external cavity length on the TDS of the generated chaotic signal is very weak for the proposed system. However, the bias current and the feedback strength seriously affect the TDS of the generated chaotic signal. In order to systematically analyze their impacts, the map of the TDS of the output chaotic signal in the parameter space of the bias current and feedback strength is displayed in Fig. 6. Here, the coupling ratio of the FC2 is 50/50, and  $L_{VDL}$  keeps 3.35 m. In this diagram, the dark blue region surrounded by dashed lines represents the TDS value lower than 0.1. Obviously, with the increase of the bias current, the dark blue region is enlarged, and the minimum value of feedback strength in the region is increased.

Finally, we analyze whether the complexity of the generated chaotic signal will be degraded after suppressing the TDS. In this work, PE is adopted to characterize the complexity of the generated chaotic signal. Here, we choose three representative operating conditions marked as points P, Q and R in Fig. 6 for discussion and the corresponding feedback strengths are 11.0%, 14.0%, and 26.0%, respectively. As shown in Fig. 6, the TDS at point P is the strongest, and the TDS at point R is the weakest. Considering that the PE values are closely related to the timescales [28], we calculate the PE values with two different  $\tau_e$ , and the results are given in Fig. 7. The blue curves are for  $\tau_e = 0.125$  ns, and the red curves are for  $\tau_e = 1.875$  ns. As shown in this diagram, for the two different timescales, obvious valleys are emerging at the feedback round-trip time  $\tau$  for point P, but there is no valley for point R. Although the values of  $\tau_e$  affect the depth of the valley, the baseline values roughly maintain at the same level. Therefore, the complexity of the chaotic signal is not reduced when the TDS is concealed.

#### IV. CONCLUSION

In summary, we propose and experimentally demonstrate a simple system for generating chaotic signals with concealed TDS. Such a system is based on a SL under MPOF which is composed of a FC and a FM. The experimental results show that the TDS of the generated chaotic signal is insensitive to the length of the feedback paths, which is convenient for practical application. Nevertheless, the TDS of the generated chaotic signal is influenced by other parameters such as the coupling ratio of the FC2 in MPOF module, the feedback strength, and the bias current, but luckily they are relatively easy to control and a large TDS concealment region has been obtained by mapping the operating parameters. Finally, the complexity of the chaotic output is estimated by the information theory based PE and the results demonstrate that the proposed MPOF scheme can effectively conceal the TDS of chaos whilst keeping high complexity chaotic output.

#### REFERENCES

- [1] D. Rontani, A. Locquet, M. Sciamanna, and D. S. Citrin, "Loss of time-delay signature in the chaotic output of a semiconductor laser with optical feedback," *Opt. Lett.*, vol. 32, no. 20, pp. 2960–2962, Oct. 2007.
- [2] J. G. Wu *et al.*, "Time delay signature concealment of optical feedback induced chaos in an external cavity semiconductor laser," *Opt. Exp.*, vol. 18, no. 7, pp. 6661–6666, Mar. 2010.

- [3] E. M. Shahverdiev and K. A. Shore, "Impact of modulated multiple optical feedback time delays on laser diode chaos synchronization," *Opt. Commun.*, vol. 282, no. 17, pp. 3568–3572, Sep. 2009.
- [4] J. G. Wu, G. Q. Xia, L. P. Cao, and Z. M. Wu, "Experimental investigations on the external cavity time signature in chaotic output of an incoherent optical feedback external cavity semiconductor laser," *Opt. Commun.*, vol. 282, no. 15, pp. 3153–3156, Aug. 2009.
- [5] S. S. Li, Q. Liu, and S. C. Chan, "Distributed feedbacks for time-delay signature suppression of chaos generated from a semiconductor laser," *IEEE Photon. J.*, vol. 4, no. 5, Oct. 2012.
- [6] S. S. Li and S. C. Chan, "Chaotic time-delay signature suppression in a semiconductor laser with frequency-detuned grating feedback," *IEEE J. Sel. Top. Quantum Electron.*, vol. 21, no. 6, Nov./Dec. 2015, Art. no. 1800812.
- [7] Y. Wu, B. J. Wang, J. Z. Zhang, A. B. Wang, and Y. C. Wang, "Suppression of time delay signature in chaotic semiconductor lasers with filtered optical feedback," *Math. Problem Eng.*, vol. 2013, pp. 1–7, Dec. 2013.
- [8] S. Y. Xiang *et al.*, "Conceal time delay signature of chaos in semiconductor lasers with dual-path injection," *IEEE Photon. Technol. Lett.*, vol. 25, no. 14, pp. 1398–1401, Jul. 2013.
- [9] N. Li, W. Pan, A. Locquet, and D. S. Citrin, "Time-delay concealment and complexity enhancement of an external-cavity laser through optical injection," *Opt. Lett.*, vol. 40, no. 19, pp. 4416–4419, Oct. 2015.
- [10] P. Mu, W. Pan, L. Yan, B. Luo, N. Li, and M. Xu, "Experimental evidence of time-delay concealment in a DFB laser with dual-chaotic optical injections," *IEEE Photon. Technol. Lett.*, vol. 28, no. 2, pp. 131–134, Jan. 2016.
- [11] P. Mu, P. He, and N. Li, "Simultaneous chaos time-delay signature cancellation and bandwidth enhancement in cascade-coupled semiconductor ring lasers," *IEEE Access*, vol. 7, pp. 11041–11048, Feb. 2019.
- [12] E. M. Shahverdiev and K. A. Shore, "Erasures of time-delay signatures in the output of an opto-electronic feedback laser with modulated delays and chaos synchronization," *IET Optoelectron.*, vol. 3, no. 6, pp. 326–330, Dec. 2009.
- [13] A. Argyris *et al.*, "Chaos-based communications at high bit rates using commercial fibre-optic links," *Nature*, vol. 438, no. 7066, pp. 343–346, Nov. 2005.
- [14] A. Uchida *et al.*, "Fast physical random bit generation with chaotic semiconductor lasers," *Nature Photon.*, vol. 2, no. 12, pp. 728–732, Dec. 2008.
- [15] I. Reidler, Y. Aviad, M. Rosenbluh, and I. Kanter, "Ultrahigh-speed random number generation based on a chaotic semiconductor laser," *Phys. Rev. Lett.*, vol. 103, no. 2, pp. 024102-1–024102-4, Jul. 2009.
- [16] Z. Ma *et al.*, "Incoherent Brillouin optical time-domain reflectometry with random state correlated Brillouin spectrum," *IEEE Photon. J.*, vol. 7, no. 4 Aug. 2015, Art. no. 6100407.
- [17] F. Y. Lin and J. M. Liu, "Chaotic radar using nonlinear laser dynamics," *IEEE J. Quantum Electron.*, vol. 40, no. 6, pp. 815–820, Jun. 2004.
- [18] J. Zhang, C. Feng, M. Zhang, Y. Liu, and Y. Zhang, "Suppression of time delay signature based on Brillouin backscattering of chaotic laser," *IEEE Photon. J.*, vol. 9, no. 2, Apr. 2017, Art. no. 1502408.
- [19] M. C. Soriano, L. Zunino, O. A. Rosso, I. Fischer, and C. R. Mirasso, "Time scales of a chaotic semiconductor laser with optical feedback under the lens of permutation information analysis," *IEEE J. Quantum Electron.*, vol. 47, no. 2, pp. 252–261, Feb. 2011.
- [20] R. M. Nguimdo, M. C. Soriano, and P. Colet, "Role of the phase in the identification of delay time in semiconductor lasers with optical feedback," *Opt. Lett.*, vol. 36, no. 22, pp. 4332–4334, Nov. 2011.
- [21] S. Li, X. Li, and S. Chan, "Chaotic time-delay signature suppression with bandwidth broadening by fiber propagation," *Opt. Lett.*, vol. 43, no. 19, pp. 4751–4754, Oct. 2018.
- [22] M. Chao *et al.*, "Permutation entropy analysis of chaotic semiconductor laser with chirped FBG feedback," *Opt. Commun.*, vol. 456, Feb. 2020, Art. no. 124702.
- [23] L. J. Quintero-Rodriguez, I. E. Zaldivar-Huerta, Y. Hong, C. Masoller, and M. W. Lee, "Permutation entropy analysis of the output of a laser diode under stimulated Brillouin scattering optical feedback," *Opt. Exp.*, vol. 29, no. 17, pp. 26787–26792, Aug. 2021.
- [24] J. G. Wu, G. Q. Xia, and Z. M. Wu, "Suppression of time delay signatures of chaotic output in a semiconductor laser with double optical feedback," *Opt. Exp.*, vol. 17, no. 22, pp. 20124–20133, Oct. 2009.
- [25] N. Jing *et al.*, "Simultaneous bandwidth-enhanced and time delay signature-suppressed chaos generation in semiconductor laser subject to feedback from parallel coupling ring resonators," *Opt. Exp.*, vol. 28, no. 2, pp. 1999–2009, Jan. 2020.
- [26] D. Chang, Z. Zhong, J. Tang, P. S. Spencer, and Y. Hong, "Flat broadband chaos generation in a discrete-mode laser subject to optical feedback," *Opt. Exp.*, vol. 28, no. 26, pp. 39076–39083, Dec. 2020.
- [27] C. Bandt and B. Pompe, "Permutation entropy: A natural complexity measure for time series," *Phys. Rev. Lett.*, vol. 88, no. 17, pp. 174102-1–174102-4, Apr. 2002.
- [28] N. Li *et al.*, "Multiscale ordinal symbolic analysis of the Lang-Kobayashi model for external-cavity semiconductor lasers: A test of theory," *IEEE J. Quantum Electron.*, vol. 51, no. 8, Aug. 2015, Art. no. 2200206.